Philosophical Magazine
Publication details, including instructions for authors and subscription information:
http://www.tandfonline.com/loi/tphm20

Heterogeneous nucleation and depletion effect in nanowire growth

F. Hodaj [a], O. Liashenko [b], A. Gusak [b] & Y. Lyashenko [b]

[a] SIMaP-UMR CNRS 5266, Grenoble INP-UJF, BP 75, F-38402, Saint Martin d'Hères, France

[b] Cherkasy National University, 81 Shevchenko blvd., Cherkasy, 18031, Ukraine

Available online: 07 Sep 2011

To cite this article: F. Hodaj, O. Liashenko, A. Gusak & Y. Lyashenko (2011): Heterogeneous nucleation and depletion effect in nanowire growth, Philosophical Magazine, DOI:10.1080/14786435.2011.607142

To link to this article: http://dx.doi.org/10.1080/14786435.2011.607142

Philosophical Magazine
2011, 1–18, iFirst

Taylor & Francis
Taylor & Francis Group

Heterogeneous nucleation and depletion effect in nanowire growth

F. Hodaj[a]*, O. Liashenko[b], A. Gusak[b] and Y. Lyashenko[b]

[a]*SIMaP - UMR CNRS 5266, Grenoble INP - UJF, BP 75, F-38402, Saint Martin d'Hères, France;* [b]*Cherkasy National University, 81 Shevchenko blvd., Cherkasy, 18031, Ukraine*

(*Received 9 May 2011; final version received 16 July 2011*)

Recent experiments by Ross and co-workers proved the possibility of a mononuclear regime with heterogeneous nucleation as well as jerky growth in the vapor–liquid–solid (VLS) process for silicon nanowires. In this work, a theoretical model is presented which incorporates the effects of (i) a mononuclear regime with layer by layer growth, (i) heterogeneous nucleation of each new layer at the edge of a Au–Si droplet, (iii) drop of supersaturation after each successful nucleation and respective fast layer growth, (iv) time-dependent nucleation barrier during each new waiting period and (v) correlation between subsequent waiting periods (non-Markovian sequence of waiting periods).

Keywords: nucleation; nanowire; modeling; thermodynamics; growth; step-flow kinetics

1. Introduction

Development of nanotechnologies provides new problems in the theory of phase transformations – nucleation, growth and coarsening in open nanosystems.

Step-flow kinetics is one of the newest experimentally investigated features of nanowire growth [1–3] by the vapor–liquid–solid (VLS) method. Nanowires grow by a rapid increase (few milliseconds) of the nanowire height by the value of one monoatomic layer with large incubation time (several seconds) between these increases. It has been shown for the II–VI or III–V compounds where solubility of one component in the liquid alloy is very low that nucleation statistics is self-regulated and corresponds to sub-Poissonian distribution of waiting times between nucleation events [3] (a similar idea was also suggested in [4]). In contrast, the solubility of Si in Au is very high and one would expect that a self-regulation mechanism will not work in such systems. Yet, nature may not meet these expectations (see below).

Growth of sufficiently thin nanowires takes place in the mononuclear regime: for the growth of one atomic layer of the nanowire it is necessary for one nucleus to appear [5]. So, here we will limit ourselves to nanosystems in which the nucleation

*Corresponding author. Email: fhodaj@simap.grenoble-inp.fr

ISSN 1478–6435 print/ISSN 1478–6443 online

DOI: 10.1080/14786435.2011.607142
http://www.informaworld.com

events proceed one by one and the probability of simultaneous nucleation and of coexistence of several nuclei is negligible. Experimental results show that a nucleus appears on the edge of the nanowire, at the junction of three phases: liquid, solid and vapor [2]. For Si nanowires grown in an atmosphere of low-pressure disilane it has been shown that the growth rate is diameter independent [6]. In this case, adsorption processes on the surface of the liquid droplet make the main contribution to the growth rate.

The following peculiarities should be taken into account in this case:

(1) 'Feedback' via depletion: in a nanovolume even one successful nucleation and subsequent monolayer growth may cause significant depletion of the whole nanosystem in one of its components [7], changing the conditions (driving force) for the next nucleation. In other words, the system should 'recover' from a previous nucleation before trying the next one.
(2) Each new nucleation event proceeds in non-steady-state conditions, under rising concentration of solute supplied by an external flux. So, the time dependence of the driving force should be taken into account [8].
(3) Time correlation: the random nucleation process is not Markovian. Each new waiting time is correlated with the previous one [3]. Indeed, if the previous waiting time was longer than the average one and the total number of incoming solute atoms was large, even after consuming atoms necessary for a new atomic layer, the system will still have a larger concentration than the average one. So, one might expect that the necessary supersaturation (for nucleation) will be reached earlier so that the next waiting time will be shorter than the average one. Thus, one might expect a negative time correlation between the nearest waiting times. Such negative time correlation should make the waiting times distribution narrower than for a common Markovian process without memory. We will investigate this phenomenon in detail below.

There are at least two experimental situations providing such a kind of nucleation process. First is the just discovered point contact reactions between nanowires of Si and metallic (Ni, Co, Pt) nanowires or nanodots, leading to jerky (stop-and-go) epitaxial growth of silicide along the silicon nanowire, each stop meaning the waiting period for nucleation of a two-dimensional (2D) island of a new silicide atomic layer [9–12]. Following the studies by Ross and co-workers we know that the same situation may be real for the VLS process [1,2].

The aim of this paper is to suggest a simple model incorporating all of the above mentioned peculiarities (mononuclear regime, depletion of the droplet by each nucleation event, stop-and-go kinetics and time correlation).

In Section 2, we present a simple model of heterogeneous nucleation of a 2D island at the triple junction droplet–wire–vapor. Namely, in Sub-section 2.1, we find the optimal shape as a function of nucleus size (number of atoms) under the conditions of mechanical equilibrium. In Sub-section 2.2, we describe the thermodynamics of 2D island nucleation at the bottom of the gold droplet taking into account depletion caused by nucleation. In addition, we will take into account depletion of the nanodroplet, which can be significant even at the nucleation stage [7] and modify the Gibbs–Thomson relations for the case of complex nucleus shape.

In Sub-section 2.3, the main equations of nucleation kinetics and lateral growth of crystalline phase are described using a simple modification of Zeldovich theory. Finally, parameters of our model are presented.

In Section 3, the results of computer experiments are presented and discussed: distribution of waiting times, time dependence of silicon concentration in liquid droplet, time correlation between subsequent waiting periods, dependence of average frequency and of average supersaturation on the flux intensity.

2. Model

Our main aim was to describe the process of layer by layer growth of a silicon nanowhisker with the help of classical nucleation theory [13], at least for the realistic case of the mononuclear regime. Successful nucleation of 2D islands to form a new layer needs sufficient supersaturation of gold with silicon. On the other hand, after successful nucleation the new layer grows fast and takes several thousands of silicon atoms causing substantial depletion of silicon in the gold droplet. (We will see below that 'depletion' actually means just a decrease of supersaturation, making the nucleation barrier too high for immediate next nucleation). If one takes the liquid droplet as a hemisphere of radius R, then the change of concentration $\Delta c_{\max}$ (molar fraction of silicon) due to attachment of one monolayer of atoms is about $\Delta c_{\max} = -\frac{\pi R^2}{(2\pi/3)R^3} = -\frac{3}{2}\frac{h}{R}$. Since the monolayer thickness h is typically a few angstroms, the concentration change can be up to 2% (for an R of about 20 nm). 'To recover' after depletion and to make a new successful nucleation attempt, the system needs time during which the whisker stands still and the droplet is gradually saturated by depositing atoms.

Actually, the theoretical scheme should depend on the hierarchy of characteristic times [14]. The total flux J is related to the deposition flux density j^{dep} by $J = j^{\text{dep}} 2\pi R^2$. First of all, one should compare the time between arrivals of new Si atoms in the droplet, $\tau_{\text{flux}} = 1/J = 1/(j^{\text{dep}} 2\pi R^2)$, the characteristic time of Si diffusion across the liquid golden droplet, $\tau_{\text{dif}} = R^2/D$, and the time for atomic layer growth to cover the whole surface after successful nucleation of a 2D island, τ_{layer}. If $\tau_{\text{flux}} \gg \tau_{\text{dif}}$, then we can apply thermodynamics for the system 'droplet plus 2D island' at a fixed number of both Au and Si atoms, considering the Si concentration as uniform in the droplet. For a nanowire (NW) radius of about 20 nm and diffusivity of Si in liquid (Au, Si) alloy D about 10^{-9} m^2 s^{-1}, the critical value of depositing flux density is $j^{\text{dep}}_{\text{crit}} \approx 10^{21}$ at. m^{-2} s^{-1}.

We consider the possibility of stoichiometric 2D island nucleation (Figure 1) (with concentration $c_i = 1$ for the case of pure Si nanowire growth) from the supersaturated liquid solution with average Si concentration c. For this we calculate the Gibbs free energy of the system $G(x)$ at different fixed number N_{Si} of Si atoms in the droplet with N_{Au} gold atoms (or fixed average concentration $c = N_{\text{Si}}/(N_{\text{Au}} + N_{\text{Si}})$) and look for the minimum in this dependence (see Figure 4a). Here x is a single parameter that characterizes the size of the nuclei; nucleus shape is determined, as usual, by mechanical equilibrium of surface tensions and by the place at which nucleation occurs (details will be shown below).

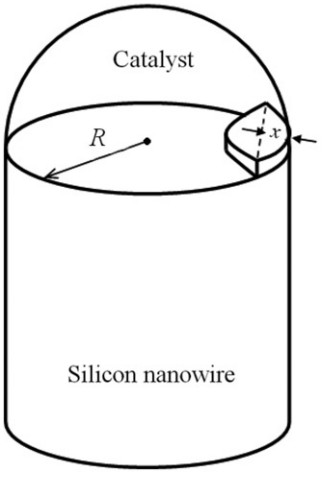

Figure 1. Model system for nanowire.

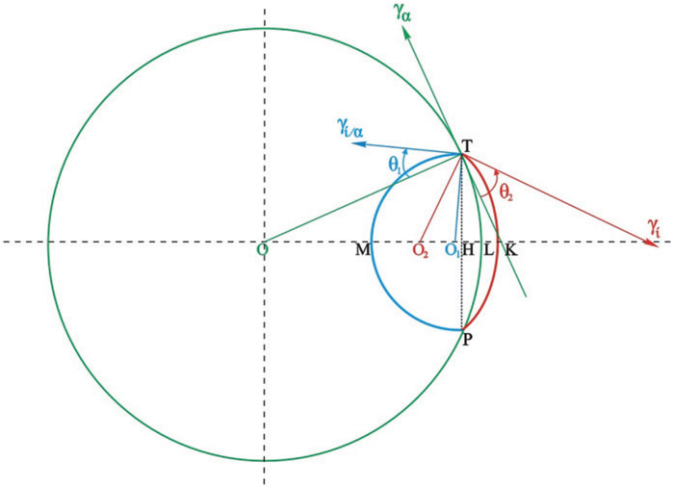

Figure 2. Shape of the nucleus and the directions of the surface tensions.

2.1. *Nucleus shape*

In our model we consider heterogeneous nucleation with a nucleus that appears on the edge of the nanowire (Figure 2). In Figure 2, O is the center of the nanowire's upper base and O_1 and O_2 are the centers of the internal and external curvatures of the nucleus, respectively.

The shape of the nucleus corresponds to the contour TMPK, which is determined by the mechanical equilibrium:

$$\begin{cases} \gamma_{i\alpha}\cos\theta_1 - \gamma_i \sin\theta_2 = 0 \\ \gamma_\alpha + \gamma_{i\alpha}\sin\theta_1 - \gamma_i\cos\theta_2 = 0. \end{cases} \tag{1}$$

γ_i, γ_α are the surface tensions of silicon (i) and Au–Si liquid phase (α) and $\gamma_{i\alpha}$ is the interfacial tension between silicon and the liquid phase.

From Equation (1) we can find values of the angles θ_1 and θ_2 for known values of γ_i, γ_α and $\gamma_{i\alpha}$

$$\theta_1 = \arcsin\left(\frac{\gamma_i^2 - \gamma_{i\alpha}^2 - \gamma_\alpha^2}{2\gamma_\alpha\gamma_{i\alpha}}\right),$$
$$\theta_2 = \arcsin\left(\frac{\gamma_{i\alpha}}{\gamma_i}\cos\theta_1\right). \tag{1'}$$

No experimental data appear to have been published on the surface tension of solid silicon (γ_i). The evaluation of γ_i by Eustathopoulos et al. [15], $\gamma_i = 1.08\,\mathrm{J\,m^{-2}}$, is in good agreement with the evaluation done elsewhere by Naidich et al. [16].

Naidich et al. [17] have measured the surface tension of liquid (Au, Si) alloys in the temperature range 364°C to about 1700°C. From their measurements, the surface tension of liquid alloys at $T = 823\,\mathrm{K}$ can be given approximately by the relation $\gamma_\alpha = 1 - 0.4c_{\mathrm{Si}}$. For a Si-saturated liquid solution at 823 K ($c_{\mathrm{Si}} \approx 0.26$) the surface tension is $\gamma_\alpha \approx 0.9\,\mathrm{J\,m^{-2}}$.

In another work, Naidich et al. [16] have studied the wetting of solid silicon by liquid Si-saturated Au–Si alloys in the temperature range 637–1573 K. Their measurements show that solid silicon is well wetted by liquid (Au,Si) alloys, the wetting contact angle (θ) being lower than about 50° whatever the temperature and the alloy composition. By analogy with liquid (Au, Ge)/solid Ge system (known surface tension of solid Ge), they took the ratio $\gamma_i/\gamma_\alpha = 1.24$. This assumption allows the authors to calculate interfacial tension $\gamma_{i\alpha}$ between solid silicon and Si-saturated (Au, Si) alloys from experimental values of contact angle (θ) and surface tension of (Au, Si) alloys (γ_α) as a function of temperature. At $T = 823\,\mathrm{K}$, the interfacial tension is $\gamma_{i\alpha} \approx 0.4\,\mathrm{J\,m^{-2}}$.

Note moreover that, in a study of anisotropy of solid Si–liquid (Al, Si) interfacial tension, Sens and Eustathopoulos [18] have shown that the maximum anisotropy $\gamma_{i\alpha}(001)/\gamma_{i\alpha}(111)$ is about 10%. For this reason and for sake of simplicity, in the following we will use constant values of interfacial tensions at $T = 823\,\mathrm{K}$:

$$\gamma_\alpha \approx 0.9\,\mathrm{J\,m^{-2}}, \quad \gamma_i = 1.08\,\mathrm{J\,m^{-2}} \quad \text{and} \quad \gamma_{i\alpha} \approx 0.4\,\mathrm{J\,m^{-2}}.$$

In our model, we vary the value of $\mathrm{HL} = x$, which allows us to fix both edges of the internal l_1 (contour TMP) and the external l_2 (contour TKP) curvatures of the nucleus. We denote the origin curvature of the nanowire bounded by these edges as l (contour TLP). For small values of x in comparison with the radius of the nanowire R we can evaluate the length of all curvatures and the area of the nucleus:

$$l = 2\sqrt{2Rx}, \quad x \ll R \tag{2}$$

$$l_1 = \frac{2(\pi/2 - \theta_1)\sqrt{2Rx}}{\cos\theta_1}, \tag{3}$$

$$l_2 = \frac{2\theta_2\sqrt{2Rx}}{\sin\theta_2}, \tag{4}$$

$$S = 2Rx\varepsilon, \tag{5}$$

where ε depends only on θ_1 and θ_2:

$$\varepsilon = \frac{(\pi/2 - \theta_1 - \sin\theta_1\cos\theta_1)}{\cos^2\theta_1} + \frac{(\theta_2 - \sin\theta_2\cos\theta_2)}{\sin^2\theta_2}. \tag{6}$$

Now we can write the dependence between x and the number of atoms in the nucleus n (from Equation (5) and $S = n\Omega/h$):

$$x = \frac{n\Omega}{2Rh\varepsilon}, \tag{7}$$

where Ω is the atomic volume.

A calculation for reasonable parameters shows that radius O_1M of internal boundary l_1 increases more rapidly than radius O_2K of external boundary l_2, so for the small nucleus (consisting of few tens of silicon atoms) we can neglect the deviation of external boundary from initial circle, and, respectively, neglect the distortion of the droplet surface in the vicinity of the nucleation site.

2.2. *Thermodynamics of nucleation and depletion in nanodroplet*

2.2.1. *Driving forces*

The change of Gibbs potential of the system at conditions of epitaxy can be defined as:

$$\Delta G = n\Delta g^{\text{bulk}} + \Delta G^{\text{surf}} = n\Delta g^{\text{bulk}} + \gamma_{i\alpha} l_1 h + \gamma_i l_2 h - \gamma_\alpha l h, \tag{8}$$

where h is the height of the monolayer and Δg^{bulk} is the bulk driving force per one atom of the nucleus (it is negative):

$$\Delta g^{\text{bulk}} = N/n[\, g(c - \Delta c) - g(c)] + g_i - g(c - \Delta c), \tag{9}$$

where $g(c)$ is the Gibbs free energy per one atom of the liquid phase (α) with concentration c, g_i is the Gibbs free energy per one atom of the solid phase with concentration $c_i = 1$ (pure silicon), Δc is the concentration depletion after the nucleus appears and N is the total number of atoms in the droplet.

Here we use experimental data and thermodynamic assessment of the Au–Si system [19,20] (see Figure 3 for the phase diagram). The Au–Si solution is modelled as a liquid solution, in which the Gibbs energies are expressed as $G = \sum_{i=\text{Au,Si}} c_i G_i^0 + RT\sum_{i=\text{Au,Si}} c_i \ln c_i + G^E$, where G_i^0 are the Gibbs energies of pure elements of Au and Si at each temperature from [19] (which are reference states for Au and Si), G^E is the excess Gibbs energy, expressed by model of subregular solution [20]. In particular, at $T = 823$ K, the expression of G is given by the following equation:

$$\begin{aligned} G[\text{J/mole}] = {} & 6702.37c - 36320.01(1-c) + 6842.42\{c\ln(c) + (1-c)\ln(1-c)\} \\ & - c(1-c)\{36562.56 + 28464.63(1-2c)\}. \end{aligned}$$

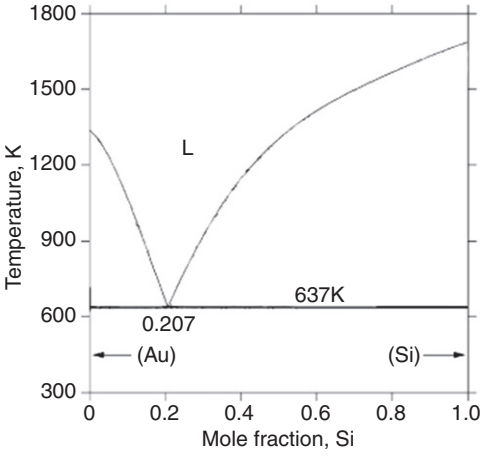

Figure 3. The Au–Si phase diagram calculated in [20].

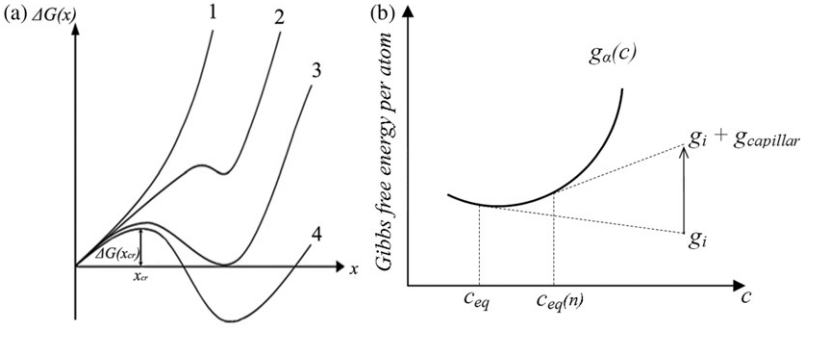

Figure 4. (a) Dependence of thermodynamic Gibbs potential of the system during nucleation. (b) Model Gibbs potentials of liquid solution and silicon (schematically).

2.2.2. *Equilibrium conditions*

We take into account the possible depletion of the droplet by the very process of 2D nucleation. In our conditions, heterogeneous nucleation occurs in the volume of metastable phase of gold–silicon liquid solution. Depending on the number of Si atoms in the droplet the following situations are possible, typical for nanoparticles and nanosize diffusion zones (see, for example, [7,21,22]):

(1) For a sufficiently small number of Si atoms (relatively small c), the Gibbs's free energy of the droplet has only one minimum corresponding to zero (see curve 1 in Figure 4a);
(2) For a larger number of Si atoms, the dependence $G(x)$ becomes non-monotonic with a second metastable minimum (see curve 2 in Figure 4a);
(3) At some critical number of Si atoms, the second minimum becomes stable (see curve 3 in Figure 4a).

After this the formation of new monolayer becomes thermodynamically favored but kinetically it depends on the height of the nucleation barrier. This height becomes smaller and smaller with the arrival of new silicon atoms inside the droplet. This means that to predict the growth characteristics we must modify the Zeldovich steady-state nucleation model [13] for the case of a non-stationary driving force.

2.2.3. *Capillary effects*

Capillary effects are usually treated in terms of curvature-dependent Laplace pressure. This is appropriate in the case of a spherical or cylindrical surface of the nucleus, otherwise direct calculation of Laplace pressure near curved interfaces may be misleading. Actually, the capillary effect will cause a size dependence of Gibbs energy, chemical potential and of the corresponding equilibrium composition. It is convenient instead of introducing individual curvatures for the different sides of the nucleus to use a single effective curvature $k^{\mathrm{ef}} = 1/R^{\mathrm{ef}}$, where R^{ef} is the effective radius of curvature, which will be introduced below.

Stable or unstable equilibrium (including the saddle-point at the nucleation barrier) is determined by the condition of zero derivative of change of Gibbs energy ΔG (see Equation (8)):

$$\begin{aligned}\frac{\mathrm{d}\Delta G}{\mathrm{d}x} &= \Delta g^{\mathrm{bulk}} + \frac{\mathrm{d}\Delta G^{\mathrm{surf}}}{\mathrm{d}n} = \Delta g^{\mathrm{bulk}} + h\left(\gamma_{i\alpha}\frac{\mathrm{d}l_1}{\mathrm{d}n} + \gamma_i\frac{\mathrm{d}l_2}{\mathrm{d}n} - \gamma_\alpha\frac{\mathrm{d}l}{\mathrm{d}n}\right)\\ &= \Delta g^{\mathrm{bulk}} + h\frac{\mathrm{d}x}{\mathrm{d}n}\left(\gamma_{i\alpha}\frac{\mathrm{d}l_1}{\mathrm{d}x} + \gamma_i\frac{\mathrm{d}l_2}{\mathrm{d}x} - \gamma_\alpha\frac{\mathrm{d}l}{\mathrm{d}x}\right),\end{aligned} \tag{10}$$

where γ^{ef} is the effective surface energy coefficient (combination of $\gamma_{i\alpha}$, γ_i and γ_α, see below).

We can find derivatives from Equations (2)–(4) and (7):

$$\frac{\mathrm{d}l}{\mathrm{d}x} = \sqrt{\frac{2R}{x}}, \quad \frac{\mathrm{d}l_1}{\mathrm{d}x} = \frac{(\pi/2-\theta_1)\sqrt{2R}}{\cos\theta_1\sqrt{x}}, \quad \frac{\mathrm{d}l_2}{\mathrm{d}x} = \frac{\theta_2\sqrt{2R}}{\sin\theta_2\sqrt{x}}, \quad \frac{\mathrm{d}x}{\mathrm{d}n} = \frac{\Omega}{2Rh\varepsilon}. \tag{11}$$

Hence,

$$\frac{\mathrm{d}\Delta G}{\mathrm{d}x} = \Delta g^{\mathrm{bulk}} + \frac{\Omega}{\sqrt{2Rx\varepsilon}}\gamma^{\mathrm{ef}} = \Delta g^{\mathrm{bulk}} + \frac{\mathrm{const}}{\sqrt{n}} = \Delta g^{\mathrm{bulk}} + g_{\mathrm{capillar}}(n) \tag{12}$$

with

$$\gamma^{\mathrm{ef}} = \frac{(\pi/2-\theta_1)}{\cos\theta_1}\gamma_{i\alpha} + \frac{\theta_2}{\sin\theta_2}\gamma_i - \gamma_\alpha, \tag{13}$$

and

$$g_{\mathrm{capillar}}(n) = \frac{\partial\Delta G^{\mathrm{surf}}}{\partial n} = \frac{\gamma^{\mathrm{ef}}\Omega}{R^{\mathrm{ef}}(n)} \tag{14}$$

with $R^{\mathrm{ef}}(n) = \sqrt{2Rx\varepsilon}$.

Thus the concentration of silicon in the droplet in equilibrium with a 2D island of size n at the edge of a nanowire surface may be found using standard common

tangent construction (Figure 4b) with rising the Gibbs energy g_i of the pure silicon by 'Laplace term' $g_{\text{capillar}}(n)$.

The change of the value of equilibrium composition $\delta c = c_{\text{eq}}(n) - c_{\text{eq}}$ (here c_{eq} corresponds to the equilibrium composition on the planar boundary) due to the appearance of curvatures on the nucleus shape should be found by use of the common tangent rule (Figure 4b):

$$\delta c = c_{\text{eq}}(n) - c_{\text{eq}} = \frac{g_{\text{capillar}}(n)}{(1-c)\,g''}, \tag{15}$$

where g'' is the curvature of the dependence $g_\alpha(C)$ at point c_{eq}.

From Equation (15) we obtain:

$$\delta c = c_{\text{eq}}(n) - c_{\text{eq}} = \frac{g_{\text{capillar}}(n)}{(1-c)\,g''} = \frac{\gamma^{\text{ef}}\Omega}{\sqrt{2Rx\varepsilon}}\frac{1}{(1-c)\,g''}. \tag{16}$$

2.3. *Kinetics*

Let us consider a kinetic model for nucleation and lateral growth of a nanowhisker, taking into account deposition flux j^{dep} of silicon atoms (in atoms of Si per m^2 of liquid surface) from disilane gas [23]:

$$j^{\text{dep}} = \frac{P}{4kT}\sqrt{\frac{8kT}{\pi m_{\text{diss}}}}, \tag{17}$$

where P is the disilane pressure and m_{diss} is the mass of disilane molecule (Si_2H_6).

In the following the molar fraction of silicon $c_{\text{Si}} = N_{\text{Si}}/(N_{\text{Si}} + N_{\text{Au}})$ will be noted by c.

The conservation law for silicon atoms in the droplet before nucleation gives:

$$\frac{\mathrm{d}N_{\text{Si}}}{\mathrm{d}t} = 2j^{\text{dep}}\pi R^2. \tag{18}$$

The rate of change of mean concentration of silicon in the droplet before the next nucleation event is approximately equal to:

$$\frac{\mathrm{d}c(t)}{\mathrm{d}t} = \frac{(1-c(t))}{N_{\text{Si}} + N_{\text{Au}}}\frac{\mathrm{d}N_{\text{Si}}}{\mathrm{d}t} = (1-c(t))\frac{3\Omega}{R}j^{\text{dep}}. \tag{19}$$

We can represent the change of mean concentration of Si discretely:

$$c(t+dt) = c(t) + (1-c(t))\frac{3\Omega}{R}j^{\text{dep}}. \tag{20}$$

Nucleation frequency can be defined as:

$$v(t) = \mathrm{e}^{-\tau/t}s(G^*, x_{\text{cr}})2\pi R, \tag{21}$$

where τ is a lag-time, necessary to reach the critical size by random walk in the size space without influence of nucleation barrier, and s is steady-state flux in the size

space (number of islands intersecting critical size per unit time per unit length of liquid/solid/vapor junction with the total length $2\pi R$). From Zeldovich theory, modified for time-dependent nucleation on the one-dimensional contour, nucleus size being determined by characteristic length x at Figure 2:

$$s = \sqrt{\frac{-\Delta G''}{\pi kT}} f^{\mathrm{eq}}(x_{\mathrm{cr}}) B(x_{\mathrm{cr}}), \tag{22}$$

where $\Delta G'' = \left(\frac{\mathrm{d}^2 \Delta G}{\mathrm{d}x^2}\right)_{x=x_{\mathrm{cr}}}$ is the curvature of the nucleation barrier, $f^{\mathrm{eq}}(x_{\mathrm{cr}})$ the equilibrium size distribution, and diffusivity of the nucleus in the size space near critical size, $B(x_{\mathrm{cr}})$, is given by:

$$B(x_{\mathrm{cr}}) = -kT \frac{\left(\frac{\mathrm{d}x}{\mathrm{d}t}\right)_{x \to x_{\mathrm{cr}}}}{\left(\frac{\mathrm{d}\Delta G}{\mathrm{d}x}\right)_{x \to x_{\mathrm{cr}}}}. \tag{23}$$

$$f^{\mathrm{eq}}(x_{\mathrm{cr}}) = \mathrm{const} \cdot \exp\left(\frac{-\Delta G(x_{\mathrm{cr}})}{kT}\right), \tag{24}$$

where $\Delta G(x_{\mathrm{cr}}) = \Delta G^*$ is a nucleation barrier, which previously (in Zeldovich theory) was treated as constant in time.

As we have a nucleus of pure silicon, each silicon atom on the triple junction could be the centre of nucleation. So, the value of const in Equation (24) can be found according to [24]:

$$\mathrm{const} = \frac{c}{\Omega^{1/3}} \frac{\mathrm{d}n}{\mathrm{d}x}. \tag{25}$$

Indeed, if the nucleus size is characterized by number of atoms then $f(n=1)$ is the number of silicon atoms at the perimeter $2\pi R$, equal to $c(2\pi R/\Omega^{1/3})$, divided by the length of that perimeter.

$$f^{\mathrm{eq}}(n=1) = \frac{c}{\Omega^{1/3}}.$$

If, instead of n, nucleus size is characterized by length x, then the distribution functions are transformed in the standard way:

$$f(x) = \frac{\mathrm{d}n}{\mathrm{d}x} f(n),$$

which immediately gives Equation (25).

2.3.1. *Determination of 'diffusivity in size space'* $\mathrm{B}(\mathrm{x_{cr}})$

2.3.1.1. *Calculation of* $\left(\frac{\mathrm{dx}}{\mathrm{dt}}\right)_{\mathrm{x} \to \mathrm{x_{cr}}}$. In this paper, we will limit ourselves to diffusion-controlled nucleation. Interface-controlled nucleation will be considered elsewhere. The critical radius (typically about 1 nm) is assumed to be much smaller than the

nanowire radius (typically 10 nm or more), so that the 2D shape of the nucleus does not prevent concentration distribution from being almost spherically symmetrical. At first we use the conservation of matter considering a 2D island surrounded by a sphere of radius sufficiently large so that in this radius can be assumed to have almost hemispherical symmetry.

Relation between total diffusion flux J^{dif} in the radial direction and the rate of nucleus growth (unusual combination of 3D diffusion with 2D particle seems OK as far as particle size is much smaller than the droplet size):

$$-J^{\mathrm{dif}} = \frac{\mathrm{d}}{\mathrm{d}t}\left(\frac{Sh}{\Omega}\right) = \frac{h}{\Omega}\frac{\mathrm{d}x}{\mathrm{d}t}\frac{\mathrm{d}S}{\mathrm{d}x}, \tag{26}$$

with

$$J^{\mathrm{dif}} = \eta j(\rho) 2\pi\rho^2 \quad \text{at any } \rho \gg x. \tag{27}$$

Factor η characterizes the deviation from spherical geometry in the vicinity of the nucleus. Unfortunately, we cannot suggest anything better than analytic solution under spherical geometry and roughly assume $\eta \approx 1/2$.

As shown in textbooks on Ham's model of precipitate growth in 3D space or for 3D ripening [25], the steady state flux density in 3D space is:

$$j(\rho) = -\frac{D\big(c - c_{\mathrm{eq}}(n)\big)}{\Omega\rho^2} r_{\min}^{\mathrm{ef}}, \tag{28}$$

where $r_{\min}^{\mathrm{ef}} = \sqrt{S/\pi}$, ($S$ is determined by Equation (5))

Moreover, from Equations (7) and (21) we obtain:

$$\frac{\mathrm{d}S}{\mathrm{d}x} = 2R\varepsilon \tag{29}$$

and

$$c - c_{\mathrm{eq}}(n) = c - c_{\mathrm{eq}} - \frac{\gamma^{\mathrm{ef}}}{\sqrt{2Rx\varepsilon}} \frac{1}{(1-c)\, g''}. \tag{30}$$

From combination of Equation (26)–(30) we obtain the growth rate:

$$\frac{\mathrm{d}x}{\mathrm{d}t} = \sqrt{\frac{2\pi}{R\varepsilon}} \frac{\eta D\left[(c - c_{\mathrm{eq}})\sqrt{x} - \frac{\Omega}{\sqrt{2R}(1-c)\, g''}\frac{\gamma^{\mathrm{ef}}}{\varepsilon}\right]}{h}. \tag{31}$$

Zero value of the growth rate corresponds to the critical size. Thus,

$$\frac{\Omega}{\sqrt{2R}(1-c)\, g''}\frac{\gamma^{\mathrm{ef}}}{\varepsilon} = (c - c_{\mathrm{eq}})\sqrt{x_{\mathrm{cr}}}. \tag{32}$$

Hence,

$$\left(\frac{\mathrm{d}x}{\mathrm{d}t}\right)_{x \to x_{\mathrm{cr}}} = \sqrt{\frac{2\pi}{R\varepsilon}} \frac{\eta D (c - c_{\mathrm{eq}})\big(\sqrt{x} - \sqrt{x_{\mathrm{cr}}}\big)}{h}. \tag{33}$$

2.3.1.2. *Calculation of* $\left(\frac{d\Delta G}{dx}\right)_{x\to x_{cr}}$. From Equation (12), and taking into account Equations (11) and (29), we obtain:

$$\frac{d\Delta G}{dx} = \frac{d\Delta G}{dn}\frac{dn}{dx} = \left(\Delta g^{bulk} + \frac{\Omega\gamma^{ef}}{\varepsilon\sqrt{2Rx}}\right)\frac{2Rh\varepsilon}{\Omega} = \Delta g^{bulk}\frac{2Rh\varepsilon}{\Omega} + \frac{h\gamma^{ef}\sqrt{2R}}{\sqrt{x}}. \tag{34}$$

The critical radius of a 2D nucleus corresponds to the zero derivative of Gibbs energy change, thus, $\Delta g^{bulk}\frac{2Rh\varepsilon}{\Omega} = -\frac{h\gamma^{ef}\sqrt{2R}}{\sqrt{x}}$. Hence,

$$\left(\frac{d\Delta G}{dx}\right)_{x\to x_{cr}} = h\gamma^{ef}\sqrt{2R}\left(\frac{1}{\sqrt{x}} - \frac{1}{\sqrt{x_{cr}}}\right) = h\gamma^{ef}\sqrt{2R}\left(\frac{\sqrt{x_{cr}} - \sqrt{x}}{x_{cr}}\right). \tag{35}$$

Finally, after substitution of Equations (33) and (35) in Equation (23), we obtain:

$$\begin{aligned} B(x_{cr}) &= -kT\sqrt{\frac{2\pi}{R\varepsilon}}\frac{\eta D(c - c_{eq})\left(\sqrt{x} - \sqrt{x_{cr}}\right)}{h}\frac{x_{cr}}{h\gamma^{ef}\sqrt{2R}\left(\sqrt{x_{cr}} - \sqrt{x}\right)} \\ &= kT\sqrt{\frac{\pi}{\varepsilon}}\frac{\eta x_{cr} D(c - c_{eq})}{Rh^2\gamma^{ef}}. \end{aligned} \tag{36}$$

Or, to avoid the simultaneous presence of the supersaturation term, $(c - c_{eq})$, and critical size parameter, x_{cr}, we can use Equation (32) once again to give:

$$B(x_{cr}) = kT\sqrt{\pi/2}\frac{\eta D\Omega}{R^{3/2}\varepsilon^{3/2}h^2(1-c)\,g''}\sqrt{x_{cr}}. \tag{37}$$

We determine nucleation probability and then use standard Monte Carlo scheme with Equation (21):

$$p(\Delta t) = v(t)\Delta t, \tag{38}$$

If, at some value t^*, *random* $< p(\Delta t)$, then

$$\overline{c}_{o,i+1} = \overline{c}_i(t^*) - \frac{3h}{2R}. \tag{39}$$

2.3.2. *Parameters and basic algorithm for modeling of step-wise nanowire growth*

Disilane pressure was varied between 1×10^{-7} and 3×10^{-5} Torr (typical values used in [1,2]), diffusivity of Si in liquid solution $D = 10^{-9}\,m^2/s$, height of monolayer $h = 0.31\times10^{-9}$ m and radius of liquid droplet (taken here approximately as hemispherical) $R = 22$ nm. The time-step was chosen depending on flux density, as one percent of anticipated average waiting time: $dt_i = \frac{\langle t\rangle_i}{100} = \frac{h}{100\Omega_i^{dep}}$.

A formulated model was used for numerical calculation of time behavior of supersaturation and step-flow kinetics. For that purpose, a Monte Carlo algorithm was used.

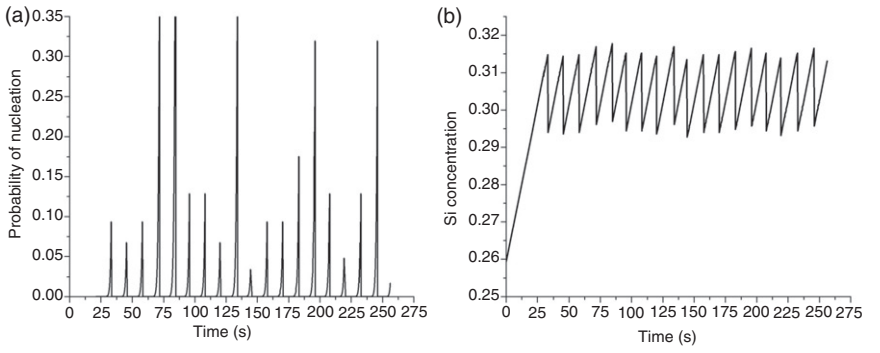

Figure 5. Typical nucleation probability dependence on time (a) and typical silicon concentration dependence on time (b) for Si nanowires with $R = 22\,\text{nm}$ grown at $T = 823\,\text{K}$ and disilane pressure $4 \times 10^{-7}\,\text{Torr}$.

3. Results and discussion

We cannot claim to predict the mean waiting time in the steady-state regime: evidently, this average time is just an inverse total flux J ($\langle t \rangle = \frac{h}{\Omega j^{\text{dep}}}$). Yet, one can suggest other characteristics. Typical time dependences of nucleation probability and of silicon content in gold droplet are presented in Figure 5. In particular, Figure 5b demonstrates that the system possesses elements of self-organization – the concentration of silicon in the droplet soon 'forgets' about its initial value and fluctuates around some steady-state asymptotic value determined by the magnitude of incoming flux: the larger the flux, the higher the average supersaturation. The dependence of the asymptotic average value of composition on incoming flux is shown in Figure 6. Time correlations between these fluctuations are discussed below.

In Figure 5b, it can also be seen that supersaturation remains significantly larger than the depletion during one monolayer growth. Indeed, the variation of silicon concentration in the drop after nucleation and 'instantaneous' growth of a silicon monolayer, for $h = 0.31\,\text{nm}$ and $R = 22\,\text{nm}$, $\Delta c_{\max} = 0.0211$ is twice as low as the mean silicon supersaturation $\overline{c} - c_{\text{eq}}$ of about 0.046. Thus, depletion as a result of nucleation, in our previous considerations, means just lower supersaturation with a respectively high nucleation barrier.

Figure 6 shows that the inverse of the supersaturation decreases linearly with the logarithm of the incoming flux density (proportional to disilane pressure). This linear character of dependence can be explained by a rather simple theoretical model to be presented elsewhere.

In Table 1, values of nucleation barrier energies for average silicon concentration (as well as the minimum and maximum values) are presented for different values of incoming flux. In this table values of average supersaturation are also reported. It can be seen that the nucleation barrier energy decreases with the increasing incoming flux, which is in agreement with the fact that silicon supersaturation increases with the deposition flux (see Figure 6a).

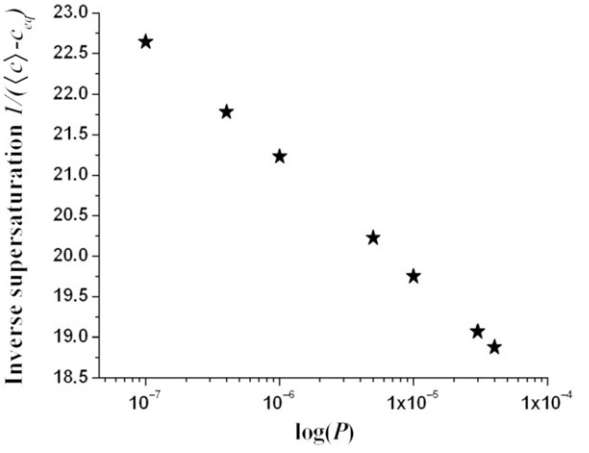

Figure 6. Dependence of inverse supersaturation on the logarithm of disilane pressure (in Torr) for Si nanowires with $R = 22$ nm grown at $T = 823$ K.

Table 1. Minimal and maximal values of nucleation barriers for $T = 823$ K.

Disilane pressure (Torr)	Average concentration	Average supersaturation	$\frac{\Delta G_{\min}}{kT}$	$\frac{\Delta G_{\max}}{kT}$
4×10^{-7}	0.3053	0.04591	27.762	36.278
5×10^{-6}	0.3088	0.04944	25.255	36.274
3×10^{-5}	0.3118	0.05244	23.573	35.319

In the Table 2 and Figures 7–8 we present:

$$\text{the average waiting time: } \langle t\rangle = \frac{\sum_{i=1}^{n} t_i}{n},$$

where the number of intervals (for successful nucleation) for each calculation is $n = 1000$;

$$\text{the square root of average squared deviation of waiting times: } \Delta = \sqrt{\frac{\sum_{i=1}^{n} (t_i - \langle t\rangle)^2}{n-1}};$$

$$\text{the dimensionless standard deviation: } d = \frac{\Delta}{\langle t\rangle};$$

$$\text{the absolute time correlation: } C = \frac{\sum_{i=2}^{n} (t_i - \langle t\rangle)(t_{i-1} - \langle t\rangle)}{n-1};$$

$$\text{and the dimensionless time correlation: } c = \frac{C}{\Delta} = \frac{\overline{(t_i - \langle t\rangle)(t_{i-1} - \langle t\rangle)}}{\overline{(t_i - \langle t\rangle)^2}}.$$

Table 2. Dependence of different time characteristics on the disilane pressure ($T = 823$ K).

Disilane pressure (Torr)	Average waiting time (s)	Average squared deviation (s)	Dimensionless standard deviation	Absolute time correlation (s)	Dimensionless time correlation
4×10^{-7}	12.456	1.238	0.099	−0.759	−0.613
5×10^{-6}	0.996	0.118	0.119	−0.007	−0.057
3×10^{-5}	0.166	0.025	0.149	-3.2×10^{-4}	−0.013

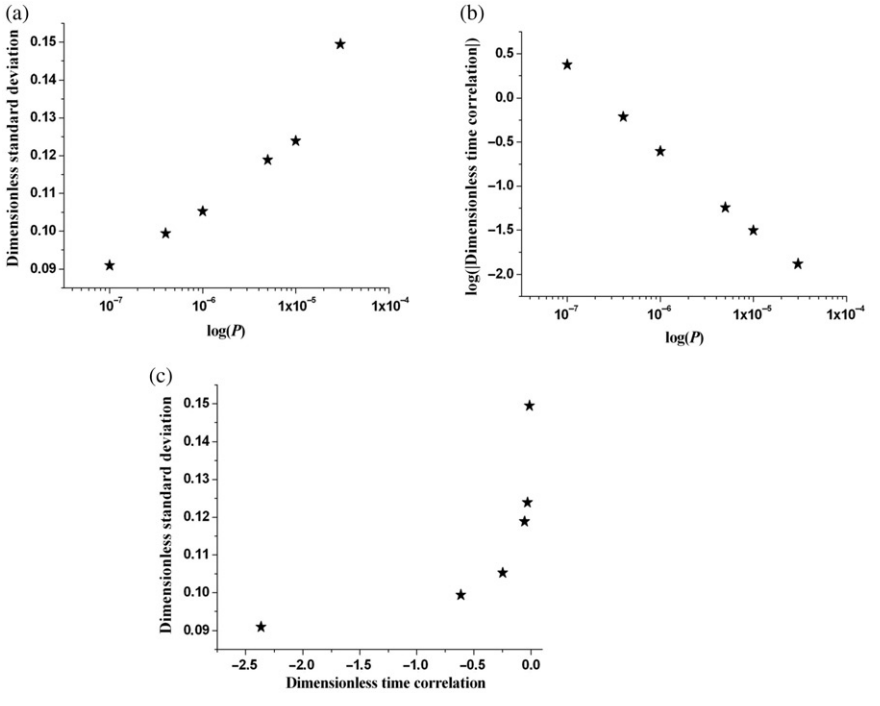

Figure 7. Dependences of dimensionless standard deviation (a) and the logarithm dimensionless time correlation (b) on the logarithm of disilane pressure (in Torr). Note that in (b) the gradient is close to –1 which means that the absolute value of the dimensionless time correlation is approximately inversely proportional to the flux density. (c) Phase-plane portrait of dimensionless standard deviation and dimensionless time correlation.

Figure 7 shows the variation of dimensionless standard deviation and dimensionless time correlation with the logarithm of deposition flux density. The dimensionless standard deviation increases almost proportionally with the logarithm of the disilane pressure (in Torr) up to 1×10^{-5} Torr, whereas the variation of dimensionless time correlation presents an asymptotic behavior (i.e. for high flux densities it tends to zero).

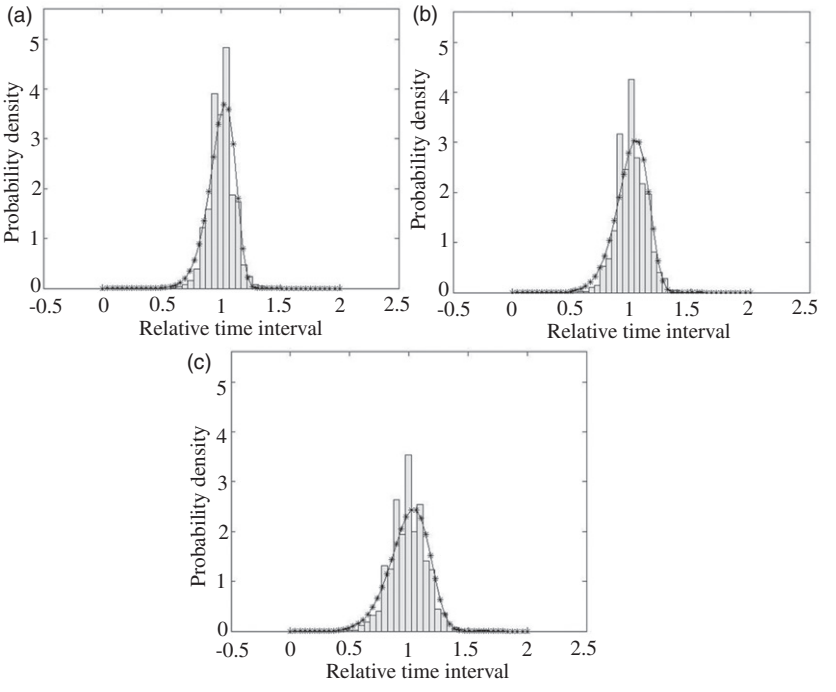

Figure 8. Distribution of waiting times fitted by Weibull distribution function: (a) for disilane pressure 4×10^{-7} Torr with parameters $a = 1.045$, $b = 10.526$; (b) for disilane pressure 5×10^{-6} Torr with parameters $a = 1.052$, $b = 8.697$; (c) for disilane pressure 3×10^{-5} Torr with parameters $a = 1.064$, $b = 7.030$.

Distributions for disilane pressures $P = 4 \times 10^{-7}$, 5×10^{-6} and 3×10^{-5} Torr are presented in Figure 8. They are rather well fitted by a Weibull distribution. Parameters of the Weibull distribution function ($y = f(x|a,b) = ba^{-b} \times x^{b-1} e^{-(\frac{x}{a})^b} I_{(0,\infty)}(x)$) are estimated. The larger the value of b, the narrower the distribution.

4. Summary

The results of this study can be summarized as follows:

(1) The possibility of jerky motion is confirmed in the model using assumptions of heterogeneous nucleation, a mononuclear mechanism and diameter-independent growth rate.
(2) Zeldovich nucleation theory (including determination of diffusivity in size space) is adapted for the case of: heterogenous nucleation; complex geometry; time-dependent driving force.
(3) Asymptotic supersaturation of liquid Au with Si increases with increasing incoming flux. Inverse supersaturation is a linear descending function of the flux density logarithm.

(4) The standard deviation of reduced waiting times distribution increases with increasing deposition flux. It correlates with the time correlation for subsequent monolayers. Stronger time correlation corresponds to narrower waiting time distribution. This result obtained for silicon repeats the conclusion of [3] for VLS growth of GaAs nanowhiskers.
(5) Waiting time correlation for subsequent events is negative and it increases by an absolute value with decreasing incoming flux. Namely, the absolute value of the dimensionless time correlation is approximately inversely proportional to the flux density.
(6) The waiting time distribution is well fitted by Weibull plots with standard deviation decreasing with decreasing flux density.

Acknowledgements

This work was supported by the DNIPRO program (EGIDE, France, and Ministry of Education and Science of Ukraine) and also by the Ukrainian State Fund for Fundamental Research.

References

[1] C.Y. Wen, J. Tersoff, M.C. Reuter, E.A. Stach and F.M. Ross, Phys. Rev. Lett. 105 (2010) p.195502.
[2] F.M. Ross, Rep. Progr. Phys. 73 (2010) p.114501.
[3] F. Glas, J.-C. Harmand and G. Patriarche, Phys. Rev. Lett. 104 (2010) p.135501.
[4] A. Gusak, A. Kovalchuk and K.N. Tu, in *Proceedings of PTM-2010,* Avignon, France, 2010, p.91. Available at http://www.ffc-asso.fr/PTM2010/fichs/doc/PTM2010-Recueil_COMPLET-31-05-2010.pdf.
[5] D. Kashchiev, Cryst. Growth Des. 6 (2006) p.1154.
[6] S. Kodambaka, J. Tersoff, M.C. Reuter and F.M. Ross, Phys. Rev. Lett. 96 (2006) p.096105.
[7] A.S. Shirinyan and A.M. Gusak, Phil. Mag. A 84 (2004) p.579.
[8] D. Kashchiev, Surf. Sci. 14 (1969) p.209.
[9] A.O. Kovalchuk, A.M. Gusak and K.N. Tu, Nano Lett. 10 (2010) p.4799.
[10] K.-C. Lu, K.N. Tu, W.W. Wu, L.J. Chen, B.-Y. Yoo and N.V. Myung, Appl. Phys. Lett. 90 (2007) p.253111.
[11] Y.-C. Lin, K.-C. Lu, W.-W. Wu, J. Bai, L.J. Chen, K.N. Tu and Y. Huang, Nano Lett. 8 (2008) p.913.
[12] Y.-C. Chou, W.-W. Wu, L.-J. Chen and K.-N. Tu., Nano Lett. 9 (2008) p.2337.
[13] L.D. Landau and E.M. Lifshitz, *Physical Kinetics*, Vol. 10, Pergamon, London, 1981.
[14] V.G. Dubrovskii, N.V. Sibirev, J.C. Harmand and F. Glas, Phys. Rev. B 78 (2008) p.235301.
[15] N. Eustathopoulos, M. Nicholas and B. Drevet, *Wettability at High Temperatures*, Vol. 3, Pergamon Materials Series, Pergamon, Oxford, 1999.
[16] Y.V. Naidich, V.M. Perevertailo and L.P. Obushchak, Poroshkavaya Metall. 5 (1975) p.73.
[17] Y.V. Naidich, V.M. Perevertailo and L.P. Obushchak, Poroshkavaya Metall. 7 (1975) p.63.
[18] H. Sens and N. Eustathopoulos, J. Cryst. Growth 98 (1989) p.751.

[19] A.T. Dinsdale, Calphad 15 (1991) p.317.
[20] F.G. Meng, H.S. Liu, L.B. Liu and Z.P. Jin, J. Alloy Comp. 431 (2007) p.292.
[21] F. Hodaj and A. Gusak, Acta Mater. 52 (2004) p.4305.
[22] A.M. Gusak, *Diffusion-controlled Solid State Reactions*, Wiley-VCH, Weinheim, 2010.
[23] K.N. Tu, *Electronic Thin-Film Reliability*, Cambridge University Press, Cambridge, 2010.
[24] V.V. Slezov and J. Schmelzer, J. Phys. Chem. Solid 55 (1994) p.243.
[25] P. Shewmon, *Diffusion in Solids*, TMS, Warrendale, PA, 1992.